Finally the remainders are combined and the last data bytes are processed, if their number is not a multiple of p. The p intermediate remainders of the last iteration and the last data bytes are combined, and divided in the classical way (Fig. 2). Again, this can be seen as an application of the preceding theorem. This step introduces a small overhead; the classical table may be used, or a binary or 'shift & add' [6] algorithm, as there will be no more than $2p-1$ bytes to process at this step.

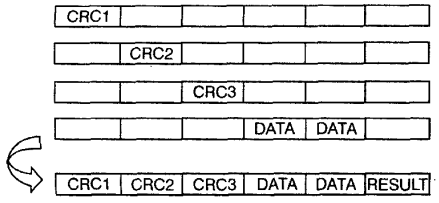

Fig. 2 *Partial CRC carry (CRC 16 bits)*

In our case, $p=6$ uses the full capacity of the memory access while giving a result every cycle (practically, this is five times faster). The resulting software pipelined loop kernel, with the LOAD and the XOR stage collapsed, is shown in Table 1.

Table 1: Piped loop kernel

Cycle	CRC1	CRC2	CRC3	CRC4	CRC5	CRC6
1	LOAD LOAD	XOR				
2		LOAD LOAD	XOR			
3			LOAD LOAD	XOR		
4				LOAD LOAD	XOR	
5					LOAD LOAD	XOR
6	XOR					LOAD LOAD

Loop control must be added
Memory access units also perform address computation

Extension: This method can be extended to the other cases ($\alpha \neq n-k$). The $\alpha > n-k$ case allows faster execution of CRC 8 at the expense of memory. It is easy to implement but not very useful in our case as α-bit words have to be read in memory, which is not possible with every value of α. It is not possible to reach $\alpha=16$ because the table cannot fit in the internal memory of the processor, and the external memory is too slow. Another drawback of $\alpha \neq 8$ is that reversed algorithms cannot be directly implemented by reversing the table values.

The most important case is $\alpha < n-k$, i.e. 16 or 32 bit polynomials with eight bits processed in parallel. The main problem in applying the same method is that the CRC is wider than one byte, which seems incompatible with the above scheme. This can be solved as follows: at each step, only the first byte of the computed CRC, that stands in the correct position, will be kept in the current polynomial. The others are ignored in the current polynomial but combined with the data bytes that have the correct position in the other polynomials (subtracted from one and added to another, see Fig. 3).

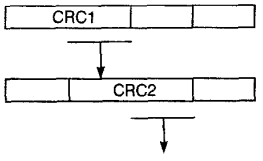

Fig. 3 *Partial CRC carry (CRC 16 bits)*

The method is easy to implement with CRC 16 bits. A single iteration of the basic algorithm takes nine cycles to complete, then we may want to execute nine parallel divisions. This is not possible owing to register pressure, and practically p is equal to 8. With careful implementation, CRC 32 also needs only two extra instructions (SHIFT and XOR), but this time it introduces an extra latency cycle leading to a data throughput of almost one byte every two cycles.

Performances: First, we can show that the VLIW DSP does not achieve substantial performance gain compared with a classical DSP ([7]), using the classical algorithm. By avoiding the LOAD dependency problem, the proposed algorithm shows a significant improvement (Fig. 4).

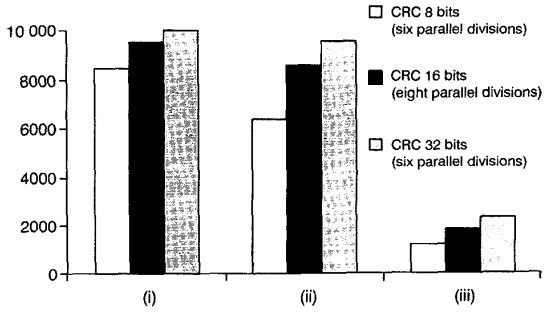

Fig. 4 *Number of cycles required to process 1024 bytes, 8 bits in parallel*

(i) TI implementation of classical algorithm on TMS320C54xx
(ii) Classical implementation on TMS320C6211 (VLIW DSP)
(iii) Proposed word-parallel algorithm on TMS320C6211

Conclusion: VLIW architectures strongly rely on the performance of the compiler, but refractory algorithms exist such as the very common CRC. The proposed method efficiently uses the TI VLIW DSP in CRC computation. It permits the efficient use of software pipelining by avoiding dependency between successive iterations, allowing processing of nearly one byte per cycle for CRC 8 and 16 bits, and one byte every two cycles for CRC 32. It should also apply to other VLIW architectures where there is memory latency.

8 October 2001
Electronics Letters Online No: 20020047
DOI: 10.1049/el:20020047

D. Hubaux and J.-D. Legat (*Microelectronics Laboratory (DICE), Université Catholique de Louvain, Place du Levant 3, 1348 Louvain-la-Neuve, Belgium*)

References

1 PEREZ, A.: 'Byte-wise CRC calculations', *IEEE Micro*, 1983, pp. 40–50
2 SARWATE, D.V.: 'Computation of cyclic redundancy checks via table lookup', *Commun. ACM*, 1988, **31**, pp. 1008–1013
3 'TMS320C6000 Tech. Brief', spru197d, Texas Instruments, 1999
4 'Optimising compiler tutorial', sprh046, Texas Instruments
5 ROGINSKY, A.L., CHRISTENSEN, K.J., and POLGE, S.: 'Efficient computation of packet CRC from partial CRCs with application to the Cells-In-Frame protocol', *Comput. Commun.*, 1998, **21**, pp. 654–661
6 FELDMEIER, D.C.: 'Fast software implementation of error detection codes', *IEEE Trans. Netw.*, 1995, pp. 640–651
7 GEREMIA, P.: 'Cyclic redundancy check computation, an implementation using the TMS320C54x'. Application Rpt spra530, Texas Instruments, 1999

Design and performance of active coupler for plastic optical fibres

J. Zubia, G. Durana, J. Arrue and I. Garcés

A simple and successful design of a new active coupler for plastic optical fibres (POF) is presented. It consists of a 2×2 coupler with a PDLC film sandwiched in it, which takes advantage of the electro-optic effect of the PDLC. More than 3 dB of variation can be achieved by applying electric fields below 1.5 V/μm.

Introduction: Currently there is a growing application of plastic optical fibres (POF) in a variety of optical links and in sensors [1,

2]. Specifically, POF are finding applications in automobiles, industrial process control, data links and other prime sectors [3]. For these applications, it is desirable to have optical devices capable of switching between two branches or of varying the power between them or of enhancing the advantages of POF with a simple and versatile design [4]. In this Letter we propose a new variable POF-based coupler that uses a polymer-dispersed liquid crystal (PDLC) film between two partially polished plastic optical fibres.

Configuration of device: The device consists of a multimode POF 2×2 coupler and a PDLC film. The 2×2 coupler was constructed by mechanically polishing off the cladding and part of the core of two pieces of POF embedded in a methacrylate block with a curved groove [4, 5]. First, a bare POF was bonded on the curved groove of the block. The groove depth at the centre of the block was approximately half the fibre diameter (0.5 mm) and the length of the polished POF section was 1 cm. The mechanical polishing was performed until the cladding and part of the core were removed and the block surface was completely smooth. Afterwards, the PDLC film was sandwiched between the two blocks of the coupler. A matching oil was applied to the interface PDLC-POF to minimise Fresnel reflections. The PDLC film was connected to a DC voltage generator by means of the transparent electrodes (ITO) of the film. A longitudinal cut of the coupler is shown in Fig. 1. The fibre used for making the coupler was a PMMA step-index 980 μm of core-diameter POF with core and cladding refractive indices given by $n_{co}=1.492$ and $n_{cl}=1.402$, respectively. The PDLC layer had a thickness around 30 μm although the entire PDLC film with ITO electrodes was slightly thicker.

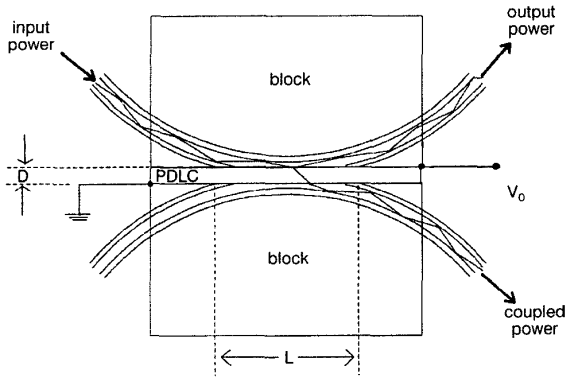

Fig. 1 *Longitudinal cut of active coupler*

Operation of device: Light is scattered when passing through an optically inhomogeneous medium. PDLC is a medium the scattered light power of which is adjustable by applying an electric field. In its uncharged state, the ordinary refractive index of the liquid crystal (n_{co}) does not match that of the polymer matrix (n_p) and the incident light is thus scattered, resulting in a translucent state. When an electric field is applied across the material, the PDLC droplets reorient and the extraordinary refractive index of the liquid crystal (n_e) matches that of the polymer. Therefore, the incident light can pass through, resulting in a transparent state. According to this, by applying a voltage to the PDLC film we can vary its transparency level and the amount of power transferred from the input branch of the coupler to the output.

Performance of device: In Fig. 2 we show the experimental results obtained for the output power of the three ports (direct port, coupled port and isolated port) against wavelength, together with the input power at the input port. This data was collected with the aid of an automatic system consisting of a lamp, a monochromator with a step motor, collimating lenses and a 20 times objective to launch the light into one of the branches of the device. The main results of the device are summarised in Table 1 for a wavelength of 612 nm and room temperature. It can be observed that the isolation increases with light wavelength, this being greater than 25 dB at 700 nm and never below 20 dB in the whole visible region. For this reason, operation in the red part of the spectrum is better. The coupling was near 3 dB although this parameter depends on the electric field applied to the PDLC film.

Fig. 3 shows the power in the coupled branch when different voltages were applied to the PDLC film. This data corresponds to a wavelength of 612 nm (in this case we used the orange line of a He-Ne laser). It can be seen that with increasing PDLC film transparency (greater voltages applied) the amount of energy coupled increased by as much as 3 dB from $V=0$ volts up to $V=50$ volts. However, for small values of the voltage, from $V=0$ volts to approximately $V=15$ volts, there was no appreciable change in the coupled power. Below this value, the electric field is not high enough to align liquid crystal droplets in the polymeric matrix. By reducing the PDLC film thickness to 10 microns, the threshold voltage can be reduced by a third or even less.

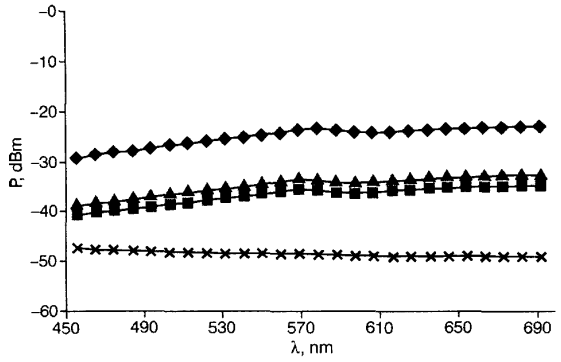

Fig. 2 *Output power at ports of coupler against wavelength*
-◆- input branch
-▲- coupled branch
-■- direct branch
-×- isolated branch

Table 1: Results of characterisation of device for $\lambda=612.0$ nm and room temperature

Coupling [%]	Excess loss	Insertion loss	Isolation	Rise time [20°C]
67	3.1 dB	4.95 dB	25 dB	400 ms

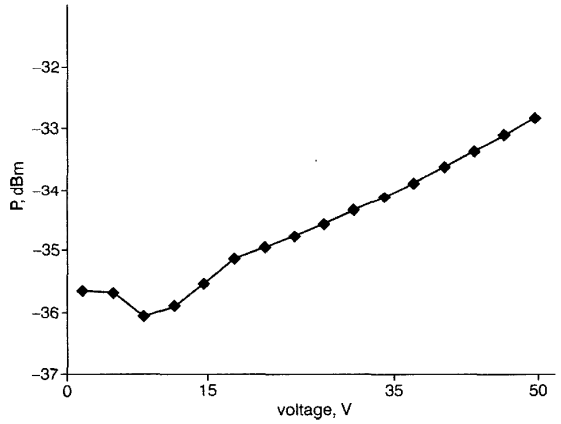

Fig. 3 *Output power at coupled branch against applied voltage*

With the aid of an oscilloscope we measured the rise and fall times of the device as well. No appreciable difference was observed between them. A mean value averaged over several cycles of 400 ms was obtained at 20°C. This value is good enough for the applications thought for the device.

Conclusions: We have developed and characterised an optical active coupler made of two polished POFs. The device shows 3.1 dB of excess losses, good uniformity between output branches and the possibility to vary the coupling by more than 3 dB by means of voltages below 1.5 V/μm. The response time, 400 ms, was good enough for the intended performance of the device.

Acknowledgment: We would like to thank Universidad del País Vasco-Euskal Herriko Unibertsitatea and Ministerio de Ciencia y Tecnología under projects 1/UPV/EHU00147.345-TA-8035/200 and TIC2000-059, for their financial support.

8 November 2001
Electronics Letters Online No: 20020062
DOI: 10.1049/el:20020062

J. Zubia, G. Durana and J. Arrue (*Departamento de Electrónica y Telecomunicaciones, Escuela Superior de Ingenieros de Bilbao, Alameda de Urkijo s/n, 48013, Bilbao, Spain*)

I. Garcés (*Departamento de Ingeniería Eléctrica, Electrónica y Comunicaciones, Centro Politécnico Superior, Maria de Luna 3, 50015, Zaragoza, Spain*)

E-mail: jtpzuzaj@bi.ehu.es

References

1 NIHEI, E., ISHIGURE, T., TANIO, N., and KOIKE, Y.: 'Present prospect of graded index plastic optical fiber in telecommunications', *IEICE Trans. Electron.*, 1997, **E-80-c**, (1), pp. 117–122
2 STEIGER, U.: 'Sensor properties and applications of POF'. Proc. Seventh International Conference on *Plastic optical fibers and applications*, Berlin, Germany, 1998, pp. 171–177
3 KOIKE, Y., ISHIGURE, T., and NIHEI, E.: 'High-bandwidth graded index polymer optical fiber', *J. Lightwave Technol.*, 1995, **13**, pp. 1475–1489
4 ZUBIA, J., IRUSTA, U., ARRUE, J., and AGUIRRE, A.: 'Design and characterisation of a plastic optical fiber active coupler', *IEEE Photonics Technol. Lett.*, 1998, **10**, (11), pp. 1578–1580
5 TSUJIMOTO, Y., SERIZAWA, H., HATORI, K., and FUKAI, M.: 'Fabrication of low loss 3 dB couplers with multimode optical fibres', *Electron. Lett.*, 1978, **14**, p. 157

Laser emission from conjugated polymer in fibre waveguide structure

T. Kobayashi and W.J. Blau

Lasing from a conjugated polymer, poly(9,9-di-(2-ethylhexyl)fluorenyl-2,7′-diyl), incorporated into a glass-clad step index optical fibre structure is reported. The fibre is fabricated by filling a glass capillary with a toluene solution containing polystyrene and the conjugated polymer. Under nanosecond transverse photopumping, the fibre 1.5 cm in length exhibits laser emission at 436 nm from a Fabry-Perot cavity formed by the Fresnel reflections at the fibre end-air interfaces.

Introduction: Conjugated polymers have been generating a great deal of interest with a view to the realisation of optically and electrically pumped organic lasers because of their clear technical advantages such as good processability, ease of chemical tailoring of emissive properties, potentially very low cost, and very large optical gain [1–3]. Ultrafast pump-probe measurements on thin films have demonstrated very large gain of the order of 10^4 cm^{-1} in some conjugated polymers [4, 5]. Furthermore, the broad emission spectrum characteristic of conjugated polymers is attractive for generation and amplification of ultrashort optical pulses.

Waveguide structures provide optical confinement and a long interaction length between the gain medium and lightwave, which are desirable for efficient operation of lasing and amplification devices. Fibre geometry is especially appealing because of its symmetric output beam pattern, scalability of output power, and the high surface-area-to-volume ratio leading to efficient heat dissipation and minimisation of thermal degradation of performance. The large gain inherent in conjugated polymers offers a possibility of constructing a very compact fibre laser having strong potential for integration with passive components in highly integrated optical networks. More importantly, such polymer fibre devices may find applications in the growing technology associated with polymer fibre-optics. The fibre waveguide structure presents compatibility for in-line interconnects within polymer optical fibre-based communication networks. Polymer fibre lasers and amplifiers operating in the visible are especially appropriate for use with polymer optical fibres as the polymer materials have their low loss windows in the visible region. For instance, a green-emitting fibre source can be potentially important because poly(methylmethacrylate), a commonly used polymer for optical fibres, has its intrinsic lowest loss region around 500 nm [6]. Despite all these appealing features, no exploitation of this class of materials has been attempted to date to realise lasers and amplifiers in a fibre form. In this Letter, we report the first demonstration of lasing from an optical fibre whose core is doped with a conjugated polymer.

Results and discussion: A step index polymer optical fibre was fabricated by using a blue-emitting conjugated polymer, poly(9,9-di-(2-ethylhexyl)fluorenyl-2,7′-diyl), as a gain medium and a glass capillary as a cladding. In the inset of Fig. 1 is shown the chemical structure of the poly(9,9-di-(2-ethylhexyl)fluorenyl-2,7′-diyl). A toluene solution containing 10 wt% of polystyrene and 3 wt% of the conjugated polymer was prepared. Then, the solution was drawn along the glass capillary 0.5 mm in inner diameter and 1.5 mm in outer diameter by capillary action. Since the refractive index of the solution (polystyrene: ~1.59, toluene: ~1.50) is higher than that of the glass tube (~1.46), the index difference provides a waveguiding effect.

The fibre 1.5 cm in length was transversely photopumped by 355 nm radiation from a frequency tripled Nd: YAG laser. The pump pulses had duration of 5 ns at a repetition rate of 10 Hz. The pump beam was focused onto a 1 mm-wide thin-striped shape on the fibre by cylindrical lenses. The output spectra from the fibre were taken with a CCD array in conjunction with a spectrometer. All the measurements were performed at room temperature.

We measured the emission from the fibre without any external resonator under nanosecond transverse photopumping. In Fig. 1, the emission intensity at the peak wavelengths is plotted against the pump energy density. A well-defined pump energy threshold is seen for the change in slope in the input-output data. This sharp threshold behaviour followed by a linear increase in output intensity is a clear signature of the occurrence of lasing. The threshold pump energy density for lasing was 1.2 mJ/cm^2 (corresponding to 240 kW/cm^2). About 4% of the Fresnel reflections at the fibre end-air interfaces acted directly as resonator mirrors.

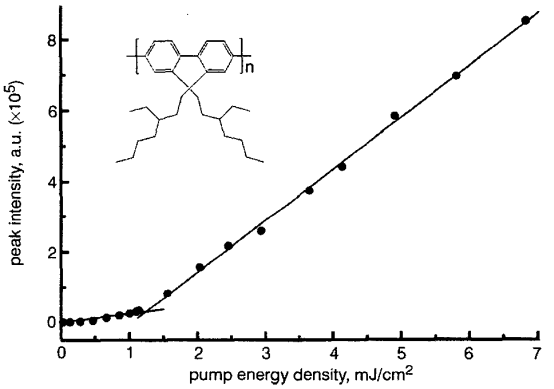

Fig. 1 *Emission intensity at peak wavelengths against pump energy density for 1.5 cm fibre*
Lasing threshold is 1.2 mJ/cm^2
Inset: Chemical structure of poly(9,9-di-(2-ethylhexyl)fluorenyl-2,7′-diyl)

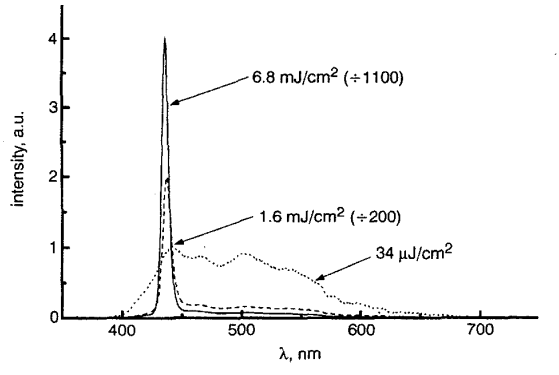

Fig. 2 *Emission spectra from fibre at different pump energy densities*

Significant spectral narrowing is another signature for lasing. Fig. 2 shows emission spectra from the fibre for different pump energy